Transportation Research Part B 43 (2009) 127–141

Contents lists available at ScienceDirect

Transportation Research Part B

journal homepage: www.elsevier.com/locate/trb

Revisiting Hughes' dynamic continuum model for pedestrian flow and the development of an efficient solution algorithm

Ling Huang [a], S.C. Wong [b,*], Mengping Zhang [a], Chi-Wang Shu [c], William H.K. Lam [d]

[a] Department of Mathematics, University of Science and Technology of China, Hefei, Anhui 230026, China
[b] Department of Civil Engineering, The University of Hong Kong, Pokfulam Road, Hong Kong, China
[c] Division of Applied Mathematics, Brown University, Providence, RI 02912, USA
[d] Department of Civil and Structural Engineering, The Hong Kong Polytechnic University, Hong Kong, China

ARTICLE INFO

Article history:
Received 19 June 2006
Received in revised form 16 June 2008
Accepted 17 June 2008

Keywords:
Pedestrian flow
Continuum modeling
Reactive dynamic user equilibrium
WENO scheme
Eikonal equation

ABSTRACT

In this paper, we revisit Hughes' dynamic continuum model for pedestrian flow in a two-dimensional walking facility that is represented as a continuum within which pedestrians can freely move in any direction [Hughes, R.L., 2002. A continuum theory for the flow of pedestrians. Transportation Research Part B, 36 (6), 507–535]. We first reformulate Hughes' model, and then show that the pedestrian route choice strategy in Hughes' model satisfies the reactive dynamic user equilibrium principle in which a pedestrian chooses a route to minimize the instantaneous travel cost to the destination. In this model, the pedestrian demand is time varying. The pedestrian density, flux, and walking speed are governed by the conservation equation. A generalized cost function is considered. The reformulated problem is solved by the efficient weighted essentially non-oscillatory scheme for the conservation equation and the fast sweeping method for the Eikonal equation. A numerical example is used to demonstrate the effectiveness of the proposed solution procedure.

1. Introduction

The continuum approach has been widely used for the macroscopic modeling of pedestrian flow. An important step in the development of a continuum model is the measurement of the macroscopic variables of pedestrian speed, density, and flow. Morrall et al. (1991) compared the walking speed on a sidewalk in Calgary with that in certain Asian cities, and found that the higher walking speed in Calgary might be due to the difference in the physical size and culture of the pedestrians or the difference between sidewalk attractions in these cities. Lam et al. (1995) measured the walking distance speed and observed the flow rate of different pedestrian facilities such as stairways, sidewalks, and signalized crossings in outdoor situations or within transit stations in Hong Kong, and found that pedestrians in Hong Kong have a slower walking speed than pedestrians in North American cities. Tanaboriboon and Guyano (1991), Koushki and Ali (1993), and Al-Masaeid et al. (1993) also studied pedestrian speed, density, and flow in Bangkok, Kuwait City, and in some developing countries. Lam et al. (1999) measured the crowding effects at rail transit stations in Hong Kong.

Based on the aforementioned findings, the relationships among the macroscopic variables of pedestrian speed, density, and flow can be established. Virkler and Elayadath (1994) comprehensively studied the relationships among these three parameters in a pedestrian tunnel using a video recording technique in which the Greenshields, bell shape, Underwood,

* Corresponding author. Tel.: +852 2859 1964; fax: +852 2559 5337.
E-mail addresses: huangl0@mail.ustc.edu.cn (L. Huang), hhecwsc@hkucc.hku.hk (S.C. Wong), mpzhang@ustc.edu.cn (M. Zhang), shu@dam.brown.edu (C.-W. Shu), cehklam@polyu.edu.hk (W.H.K. Lam).

0191-2615/$ - see front matter © 2008 Elsevier Ltd. All rights reserved.
doi:10.1016/j.trb.2008.06.003

Greenberg, Edie, 2-regime linear, and 3-regime linear speed–density models were tested. Lam et al. (1995) investigated the relationships among speed, density, and flow for various kinds of pedestrian facilities such as walkways, stairways in transit stations, and crosswalks, and stated that different kinds of speed–density models should be adopted for different pedestrian facilities, and that no single model fits all facilities. Daly et al. (1991), Al-Masaeid et al. (1993), Cheung and Lam (1998), Lam and Cheung (1998, 2000), and Harris (1991) conducted similar studies of the relationships among speed, density, and flow in a pedestrian stream. More recently, Lam and Cheung (1997) and Lam et al. (2002, 2003a) studied the interactions within bidirectional pedestrian flows of walking facilities such as indoor walkways and signalized crosswalks in Hong Kong.

The route choice behavior of pedestrians was studied by Cheung and Lam (1998), who aimed to model the pedestrian route choice between escalators and stairways within Mass Transit Railway (MTR) stations in Hong Kong. A logit-type choice model that was based on the discomfort measure of the chosen facility was used for modeling pedestrian choices between stairways and escalators. Cheung and Lam suggested that the discomfort measure of a facility was the sum of the time spent accessing and using that facility. This choice model was then calibrated by survey data from the MTR stations. It was found that pedestrians were less sensitive to a relative delay when using the escalator, as extra effort was required from them if they chose to use the stairway. Dernellis and Ashworth (1994) modeled the route choice behavior of pedestrians, and determined the influence of factors such as the nearside traffic flow, distance, and time ratio between the subway and surface route on pedestrian choices of subway usage. Based on survey data, they found that the nearside traffic flow was linearly related to the proportion of subway users, and that a higher nearside traffic flow rate increased the proportion of subway usage. However, for the distance and time ratios, logit choice models were suggested for evaluating the proportion of subway users. In these two logit models, the proportion of subway usage decreased as the distance or time of the subway route increased. Lam et al. (2003b) studied the wayfinding problem in the passenger terminal of the Hong Kong International Airport. These studies point to the importance of route choice behavior in the macroscopic modeling of pedestrian flow problems.

Recently, a promising approach has been developed to model route choice behavior in the two-dimensional continuum modeling of user equilibrium problems, with wide-ranging applications, for example, to the multi-commodity cost–flow relationship (Wong, 1998), market share determination (Wong and Yang, 1999; Loo et al., 2005), elastic market externalities (Yang and Wong, 2000), the cordon-based congestion pricing problem (Ho et al., 2005), the combined distribution and assignment model (Wong and Sun, 2001; Wong et al., 2004), the combined discrete and continuum model (Wong, 1994; Wong et al., 2003), the multiclass user equilibrium model (Ho et al., 2004, 2006, 2007), and the housing problem (Ho and Wong, 2007). As pedestrians can freely move in the two-dimensional domain of the walking facility, the application of this continuum approach is a promising way to model the route choice behavior of pedestrians in the context of the macroscopic modeling of pedestrian flow problems.

The continuum approach mentioned above focuses on the steady-state paradigm. Recently, the dynamic modeling of pedestrian flow problems has received much attention. Selim and Al-Rabeh (1991) modeled pedestrian flow on a bridge to provide insights for bridge design, whereby the number of pedestrians who were interested in accessing the bridge varied over time. By considering the capacity of the bridge and minimizing the cost/penalty function, they found that the optimal number of pedestrians admitted to access the bridge varied over time. With this finding, valuable information was gained for the control strategy of pedestrian flow on bridges. Setti and Hutchinson (1994) introduced a passenger-terminal simulation model for airports in which a fluid approximation approach was adopted to model the passenger flow characteristics. Buckman and Leather (1994) modeled transit station congestion by using the PEDROUTE passenger simulation model.

In the continuum modeling context, Hughes (2002) provided a systematic framework for the dynamic macroscopic modeling of pedestrian flow problems. However, the user equilibrium concept is not explicitly discussed and a numerical solution procedure is not provided. To describe the route choice strategy of pedestrians, Hoogendoorn et al. (2003) and Hoogendoorn and Bovy (2004a,b) developed a predictive user equilibrium model for describing the dynamic route choice behavior of pedestrians in which pedestrians were assumed to have perfect information to make their route choice decisions over time. This modeling approach is useful in representing a more strategic level of route choice decision making whereby pedestrians accumulate travel information from their daily experience or other sources, so that they can fully anticipate the changes in the operating conditions of the walking facility. However, in some situations, pedestrians may not be familiar with the characteristics and behavior of the crowd around them, and thus it may be difficult for them to anticipate the likely responses of other pedestrians to the facility over time. In such cases, it may be appropriate to use a reactive user equilibrium model in which pedestrians need only evaluate the immediate operating conditions of the walking facility at the time they are making route decisions (see Tong and Wong (2000) for the difference between predictive and reactive dynamic user equilibrium principles).

In this paper, we revisit and reformulate Hughes' model and discover that the pedestrian route choice strategy in Hughes' model satisfies the reactive dynamic user equilibrium principle in which a pedestrian chooses a route to minimize the instantaneous travel cost to the destination. This offers a useful foundation for the application of Hughes' model when pedestrians do not have predictive information when making a route choice decision, and must rely on instantaneous information and make choices in a reactive manner while walking through the facility. However, in both of the aforementioned reactive and predictive models, we need to assume that the walking facility is fully visible to pedestrians, so that pedestrians can make corresponding decisions based on the present (reactive) or future (predictive) pedestrian flow conditions.

The rest of the paper is organized as follows. Section 2 summarizes Hughes' original dynamic continuum model for pedestrian flow. Section 3 reformulates this model and shows that the route strategy satisfies the reactive dynamic user

equilibrium principle. Section 4 derives an efficient solution algorithm for the model, and Section 5 presents a numerical example to demonstrate the effectiveness of the proposed solution procedure. Section 6 concludes the paper and suggests future research directions.

2. Hughes' original model

In Hughes (2002), a two-dimensional walking facility is considered to be a continuum with a domain Ω. The boundary of the continuum, Γ, comprises three classes of segments, $\Gamma_o \subset \Gamma$, $\Gamma_d \subset \Gamma$, and $\Gamma_h \subset \Gamma$, so $\Gamma = \Gamma_o \cup \Gamma_d \cup \Gamma_h$. The origin segment Γ_o represents the boundary at which pedestrians enter the walking facility, the destination segment Γ_d represents the boundary at which pedestrians leave the facility, and Γ_h represents the hard boundary at which no pedestrians are allowed to enter or leave the facility. The time horizon of analysis is T. Let $v_1(x,y,t)$ and $v_2(x,y,t)$ be the pedestrian speed at location (x,y) at time t in the x and y directions, respectively.

Similar to many physical systems, the speed, flow, and density of pedestrians are governed by the flow conservation equation,

$$\rho_t(x,y,t) + \nabla \cdot (\rho(x,y,t)\mathbf{v}(x,y,t)) = 0, \tag{1}$$

where $\rho(x,y,t)$ is the pedestrian density at location (x,y) at time t, $\mathbf{v}(x,y,t) = (v_1(x,y,t),\ v_2(x,y,t))$ is the speed vector, $\rho_t(x,y,t) = \partial\rho(x,y,t)/\partial t$, and $\nabla \cdot (\rho(x,y,t)\mathbf{v}(x,y,t)) = \partial\,(\rho(x,y,t)v_1(x,y,t))/\partial x + \partial(\rho(x,y,t)v_2(x,y,t))/\partial y$.

Then, Hughes defines a potential function, $\phi(x,y,t)$, and assumes that a pedestrian at location (x,y) at time t will move in a direction perpendicular to the isopotential curve at that location, i.e.,

$$\hat{\phi}_1(x,y,t) = \frac{-\phi_x(x,y,t)}{\|\nabla\phi(x,y,t)\|}, \quad \hat{\phi}_2(x,y,t) = \frac{-\phi_y(x,y,t)}{\|\nabla\phi(x,y,t)\|}, \tag{2}$$

where $\hat{\phi}_1(x,y,t)$ and $\hat{\phi}_2(x,y,t)$ are the direction cosines of the motion, $\phi_x(x,y,t) = \partial\phi\,(x,y,t)/\partial x$ and $\phi_y(x,y,t) = \partial\phi(x,y,t)/\partial y$, and $\|\nabla\phi\,(x,y,t)\| = (\phi_x(x,y,t)^2 + \phi_y(x,y,t)^2)^{1/2}$. Therefore,

$$v_1(x,y,t) = u(x,y,t)\hat{\phi}_1(x,y,t), \quad v_2(x,y,t) = u(x,y,t)\hat{\phi}_2(x,y,t), \tag{3}$$

where $u(x,y,t)$ is the isotropic pedestrian speed at location (x,y) at time t, which is a function of density and is location dependent, i.e.,

$$u(x,y,t) := U(\rho(x,y,t),x,y). \tag{4}$$

To account for the discomfort effect, Hughes defines a function

$$g(x,y,t) := G(\rho(x,y,t),x,y) \tag{5}$$

that describes the behavior of a pedestrian to avoid high density crowds, which satisfies the following equation:

$$\frac{1}{\|\nabla\phi(x,y,t)\|} = g(x,y,t)\|\mathbf{v}(x,y,t)\| = g(x,y,t)u(x,y,t). \tag{6}$$

The functions $U(\rho(x,y,t),x,y)$ and $G(\rho(x,y,t),x,y)$ have the following properties in Hughes (2002):

$$U(0) \text{ is finite}, \quad U(\rho_{\max}) = 0, \quad \frac{\partial U(\rho)}{\partial\rho} \leqslant 0, \tag{7}$$

$$G(\rho) \geqslant 1, \quad \frac{\partial G(\rho)}{\partial\rho} \geqslant 0. \tag{8}$$

Eqs. (1)–(8) constitute the original model of Hughes (2002), which is useful for describing the movement of large crowds, as a crowd generally moves as an entity and individual differences are less important (Gaskell and Benewick, 1987). In this model, it is assumed that tall pedestrians have a clear view of the operating conditions of the whole walking facility, and that short pedestrians obtain such information from or follow the route decisions of neighboring taller pedestrians. However, the model does not require that pedestrians anticipate the changes in the operating conditions over time. The model intends to describe the aggregate behavior of a homogeneous crowd with a common goal, such as the crowd movement in a railway platform or at a sporting event, holy site, or political demonstration, rather than the heterogeneous behavior of individuals, which can be studied using the microscopic simulation approach (Helbing et al., 2005). This approach is analogous to the widely used Lighthill–Whitham–Richard (LWR) macroscopic modeling approach for road traffic, which serves as a good first-order approximation of the traffic movement on a unidirectional highway (Lighthill and Whitham, 1955; Richards, 1956).

Hughes' model is built on three hypotheses: (A) the speed of pedestrians is determined by the local density around them (Eq. (4)), (B) a potential field exists such that pedestrians move at right angles to lines of constant potential (Eq. (2)), and (C) pedestrians seek the path that minimizes their (estimated) travel time, but temper this behavior to avoid extremely high densities (Eq. (6)). However, the physical interpretation of the potential field and the route strategy of pedestrians in a crowd are not explicitly revealed in Hughes (2002). In the following section, we reformulate Hughes' model and show that the

potential function can be interpreted as the instantaneous total cost to the destination, thus demonstrating that the route strategy in Hughes' model satisfies the reactive dynamic user equilibrium principle.

3. Reformulation of Hughes' model

Let $\mathbf{f}(x,y,t) = (f_1(x,y,t), f_2(x,y,t))$ be the vector of the flux in the walking facility, where $f_1(x,y,t)$ is the flux in the x-direction, and $f_2(x,y,t)$ is the flux in the y-direction. By default, $f_1(x,y,t) = f_2(x,y,t) = 0$ on Γ_h, and

$$f_1(x,y,t) = \rho(x,y,t)v_1(x,y,t), \quad f_2(x,y,t) = \rho(x,y,t)v_2(x,y,t), \tag{9}$$

$$\|\mathbf{f}(x,y,t)\| = u(x,y,t)\rho(x,y,t), \tag{10}$$

where $\|\mathbf{f}(x,y,t)\| = (f_1(x,y,t)^2 + f_2(x,y,t)^2)^{1/2}$. Substituting Eq. (9) into Eq. (1), the conservation equation becomes

$$\rho_t(x,y,t) + \nabla \cdot \mathbf{f}(x,y,t) = 0, \tag{11}$$

where $\nabla \cdot \mathbf{f}(x,y,t) = \partial f_1(x,y,t)/\partial x + \partial f_2(x,y,t)/\partial y$.

We further define $c(x,y,t)$ as the local cost per unit distance of movement at time $t \in T$ in the facility, which depends on the local operating conditions in the walking facility,

$$c(x,y,t) := C(\rho(x,y,t), x, y, t), \tag{12}$$

which can be location and time dependent to represent pedestrian behavior such as the preference for walking away from the boundary and the value placed on time at different times of day.

To ensure that pedestrians from a given location $(x,y) \in \Omega$ will choose a path that minimizes their individual walking cost to the destination, based on the instantaneous travel cost information that is available at the time of decision making, we require that

$$c(x,y,t)\frac{\mathbf{f}(x,y,t)}{\|\mathbf{f}(x,y,t)\|} + \nabla\phi(x,y,t) = 0. \tag{13}$$

From Eq. (13), we can observe the following property (see Wong et al., 1998):

$$\mathbf{f}(x,y,t) // -\nabla\phi(x,y,t), \tag{14}$$

where // indicates that the two vectors are parallel and point in the same direction. In other words, the vector of the flux points in the opposite direction of the gradient of the cost potential. In addition, we show that

$$c(x,y,t) = \|\nabla\phi(x,y,t)\|, \tag{15}$$

which is called the Eikonal equation and is discussed in Section 4.

For any used path p from location $(x,y) \in \Omega$ to destination $(x_0,y_0) \in \Gamma_d$, if we integrate the local walking cost along the path, then the total cost incurred by pedestrians can be obtained as

$$\Pi_p(x,y,t) = \int_p c(x,y,t)\mathrm{d}s = \int_p c(x,y,t)\frac{\mathbf{f}(x,y,t)}{\|\mathbf{f}(x,y,t)\|}\cdot\mathbf{ds} = -\int_p \nabla\phi(x,y,t)\cdot\mathbf{ds} = -(\phi(x_0,y_0,t) - \phi(x,y,t)) \tag{16}$$

using Eqs. (13)–(15) and given that $\mathbf{f}(x,y,t)/\|\mathbf{f}(x,y,t)\|$ is a unit vector that is parallel to $\mathbf{ds}$ along the path. Hence, the total instantaneous walking cost at time $t \in T$ is independent of the used paths.

In contrast, for any unused path $\tilde{p}$ between a location $(x,y) \in \Omega$ to the destination $(x_0,y_0) \in \Gamma_d$, the total cost that is incurred by pedestrians is

$$\Pi_{\tilde{p}}(x,y,t) = \int_{\tilde{p}} c(x,y,t)\mathrm{d}s \geqslant \int_{\tilde{p}} c(x,y,t)\frac{\mathbf{f}(x,y,t)}{\|\mathbf{f}(x,y,t)\|}\cdot\mathbf{ds} = -\int_{\tilde{p}} \nabla\phi(x,y,t)\cdot\mathbf{ds} = -(\phi(x_0,y_0,t) - \phi(x,y,t)) \tag{17}$$

using Eqs. (13)–(15). The inequality in the above derivation occurs because for some segments along path $\tilde{p}$, the normal vectors $\mathbf{f}(x,y,t)/\|\mathbf{f}(x,y,t)\|$ and $\mathbf{ds}$ are not parallel, and thus $ds > (\mathbf{f}/\|\mathbf{f}\|)\cdot\mathbf{ds}$ for those segments. Hence, for any unused paths, the total instantaneous walking cost is greater than or equal to that of the used paths.

If we set $\phi(x,y,t) = 0\ \forall (x,y) \in \Gamma_d$, then $\phi(x_0,y_0,t) = 0$, and thus $\phi(x,y,t)$ can be interpreted as the minimum instantaneous travel cost to the destination. In this way, the model guarantees that pedestrians will choose their paths in the walking facility in a user-optimal manner with respect to the instantaneous walking cost information, that is, the pedestrian flow conditions at the time.

Now, if we take the following specific form:

$$C(\rho(x,y,t), x, y, t) := \frac{1}{U(\rho(x,y,t), x, y)G(\rho(x,y,t), x, y)}, \tag{18}$$

then from Eq. (13),

$$\frac{\mathbf{f}(x,y,t)}{\|\mathbf{f}(x,y,t)\|} = -u(x,y,t)g(x,y,t)\nabla\phi(x,y,t). \tag{19}$$

Substituting Eqs. (9) and (10) into Eq. (19), we have

$$\mathbf{v}(x,y,t) = -u(x,y,t)^2 g(x,y,t)\nabla\phi(x,y,t). \tag{20}$$

Taking the norm on both sides and given that $\|\mathbf{v}(x,y,t)\| = u(x,y,t)$,

$$\|\nabla\phi(x,y,t)\| = \frac{1}{u(x,y,t)g(x,y,t)}, \tag{21}$$

which is Eq. (6) in Hughes' model. Combining Eqs. (20) and (21), we show that

$$\mathbf{v}(x,y,t) = u(x,y,t)\frac{-\nabla\phi(x,y,t)}{\|\nabla\phi(x,y,t)\|}, \tag{22}$$

which constitutes exactly Eqs. (2) and (3) in Hughes' model. Therefore, Hughes' model satisfies the reactive user equilibrium principle if the generalized cost takes the form given in Eq. (18). In other words, we can interpret the route strategy in Hughes' model as that which minimizes the instantaneous perceived (discounted due to the discomfort effect) travel time to the destination in a reactive manner, in which the function $G(\cdot)$ is the discount factor of the actual speed when perceived by pedestrians. Note that in Hughes' model, the discomfort function $G(\cdot)$ is assumed to be an increasing function of density (see Eq. (8)), which means that pedestrians will perceive that a crowd of higher density will move faster when making reactive route decisions. This is counterintuitive, and thus a more realistic form of the discomfort function is that $G(\cdot)$ is a decreasing function of density, i.e.,

$$\frac{\partial G(\rho)}{\partial\rho} \leqslant 0. \tag{23}$$

Furthermore, the functional form of the generalized cost in Eq. (18) is too restrictive in describing the route choice behavior of pedestrians, even in the context of reactive dynamic use equilibrium conditions. Therefore, a more general modeling structure can be defined by the following set of differential equations:

$$\rho_t(x,y,t) + \nabla\cdot\mathbf{f}(x,y,t) = 0 \quad \forall(x,y)\in\Omega,\ \ t\in T, \tag{24}$$

$$U(\rho(x,y,t),x,y)\rho(x,y,t) = \|\mathbf{f}(x,y,t)\| \quad \forall(x,y)\in\Omega,\ \ t\in T, \tag{25}$$

$$C(\rho(x,y,t),x,y,t)\frac{\mathbf{f}(x,y,t)}{\|\mathbf{f}(x,y,t)\|} + \nabla\phi(x,y,t) = 0 \quad \forall(x,y)\in\Omega,\ \ t\in T, \tag{26}$$

where Eq. (24) is the conservation equation, Eq. (25) is the definitional equation (10) that describes the direct relationship between density and flux, and Eq. (26) is a more generalized form of the route strategy in which pedestrians choose the instantaneous minimum cost route according to the generalized cost function $C(\rho(x,y,t),x,y,t)$. Note that Eq. (26) is the main physical equation governing cost potential ϕ, whereas Eikonal equation (15) that can be derived from Eq. (26) is an intermediate step to obtain the numerical solution in Section 4. In Section 5, we use a generalized cost function that is a linear combination of the actual travel time and the level of discomfort in a numerical example to demonstrate the versatility of this reformulation to handle the more general route choice behavior of pedestrians.

To complete the reformulation, the system in Eqs. (24)–(26) is subject to the initial boundary conditions

$$\mathbf{f}(x,y,t)\cdot\mathbf{n}(x,y) = q(x,y,t) \quad \forall(x,y)\in\Gamma_o,\ \ t\in T, \tag{27}$$

$$\rho(x,y,0) = \rho_0(x,y) \quad \forall(x,y)\in\Omega, \tag{28}$$

$$\phi(x,y,t) = 0 \quad \forall(x,y)\in\Gamma_d,\ \ t\in T, \tag{29}$$

where $q(x,y,t)$ is the time-varying pedestrian demand on the origin segments, which represents the number of pedestrians who cross a unit width of the origin segment, $\mathbf{n}(x,y)$ is a unit normal vector that points to the domain Ω, and $\rho_0(x,y)$ is the initial pedestrian density at time $t = 0$. The potential in Eq. (29) can be set to any arbitrary constant, but setting it to zero has the advantage that the resultant solution $\phi(x,y,t)\ \forall(x,y)\in\Omega$ is exactly the instantaneous minimum cost from the location (x,y) to the destination at time t.

The mathematical properties of the system, such as the supercritical and subcritical flows and conformal invariance of equations, are thoroughly discussed in Hughes (2002). In addition, if the vector flux $\mathbf{f}$ in Eq. (24) is an algebraic function of the density ρ, then the existence and uniqueness of the entropy solution to the scalar conservation law (24) is well known, see, e.g., LeVeque (1992). Likewise, the existence and uniqueness of the viscosity solution of the Hamilton–Jacobi equation (15) for a given function $c(x,y,t)$ is well known, see, e.g., Crandall and Lions (1983). However, the properties of the solutions to the coupled partial differential equations (15) and (24)–(26) such as their existence, uniqueness, and time growth are not known. Our numerical simulation results in Section 5 suggest that the solutions to this set of coupled equations are well behaved, but a rigorous mathematical study is not provided in this paper.

4. Solution algorithm

In this section, we describe an efficient solution method for the pedestrian model, which includes the fifth-order weighted essentially non-oscillatory (WENO) scheme that we use to solve the conservation law equation (24), the fast

sweeping method based on the third-order WENO scheme that we use to solve the Eikonal equation (15), and the third-order total-variation-diminishing (TVD) Runge–Kutta time discretization that we use to solve the coupled system of equations.

4.1. The WENO scheme

In this subsection, we briefly summarize high-order WENO schemes (Liu et al., 1994; Jiang and Shu, 1996), which are popular schemes in many applications, such as in computational fluid dynamics (CFD), for simulating flows with discontinuous solutions (Shu, 2003). WENO schemes have also been applied to the simulation of traffic flow models, e.g., in Zhang et al. (2003). The basic idea of a WENO scheme is the locally adaptive choice of the approximation stencil, so that high-order accuracy is achieved in smooth regions and discontinuities are resolved in a sharp and non-oscillatory fashion. We use the fifth-order WENO scheme of Jiang and Shu (1996) to approximate the conservation law equation (24) after the flux values **f** have been obtained.

The semi-discrete version of the fifth-order WENO scheme approximates the point values $\rho_{i,j} \approx \rho(x_i, y_j, t)$ of Eq. (24) through a conservative difference formula

$$\frac{\mathrm{d}}{\mathrm{d}t}\rho_{ij} = -\frac{1}{\Delta x}\left((\hat{f}_1)_{i+\frac{1}{2}j} - (\hat{f}_1)_{i-\frac{1}{2}j}\right) - \frac{1}{\Delta y}\left((\hat{f}_2)_{ij+\frac{1}{2}} - (\hat{f}_2)_{ij-\frac{1}{2}}\right), \tag{30}$$

where Δx and Δy are the mesh sizes in x and y, respectively, which are assumed to be uniformly $\Delta x = \Delta y = h$ for simplicity. $(\hat{f}_1)_{i+\frac{1}{2}j}$ and $(\hat{f}_2)_{ij+\frac{1}{2}}$ are the numerical fluxes in the x and y directions, respectively. We describe the details of the definition of the x flux $(\hat{f}_1)_{i+\frac{1}{2}j}$ below. The definition for the y flux $(\hat{f}_2)_{ij+\frac{1}{2}}$ is analogous. When we are computing the x fluxes $(\hat{f}_1)_{i+\frac{1}{2}j}$, the y index j is *fixed*. Therefore, for simplicity of notation, we drop the y index j below when there is no confusion.

We first assume $f_1'(\rho) \geqslant 0$, namely, a positive wind direction, to simplify the description. The general case is commented upon later. In this case, the numerical flux $(\hat{f}_1)_{i+\frac{1}{2}j}$ is obtained through a one-point upwind-biased stencil containing $s_\ell = f_1(x_\ell, y_j, t)$ for $\ell = i-2, i-1, \ldots, i+2$. First, we form the following three third-order numerical fluxes based on three different sub-stencils given by

So, since the value of S goes from i-2 to i+2, it's a fifth order method.

$$\begin{aligned}
\hat{s}^{(1)}_{i+\frac{1}{2}} &= \tfrac{1}{3}s_{i-2} - \tfrac{7}{6}s_{i-1} + \tfrac{11}{6}s_i,\\
\hat{s}^{(2)}_{i+\frac{1}{2}} &= -\tfrac{1}{6}s_{i-1} + \tfrac{5}{6}s_i + \tfrac{1}{3}s_{i+1},\\
\hat{s}^{(3)}_{i+\frac{1}{2}} &= \tfrac{1}{3}s_i + \tfrac{5}{6}s_{i+1} - \tfrac{1}{6}s_{i+2}.
\end{aligned} \tag{31}$$

We then define the three nonlinear weights ω_m for $m = 1, 2, 3$, by

$$\omega_m = \frac{\tilde{\omega}_m}{\sum_{l=1}^{3}\tilde{\omega}_l}, \quad \tilde{\omega}_l = \frac{\gamma_l}{(\varepsilon + \beta_l)^2}, \tag{32}$$

where the linear weights γ_l are given by

$$\gamma_1 = \frac{1}{10}, \quad \gamma_2 = \frac{3}{5}, \quad \gamma_3 = \frac{3}{10}, \tag{33}$$

and the smoothness indicators β_l, which measure the smoothness of the approximation in the lth substencil, are given by

$$\begin{aligned}
\beta_1 &= \frac{13}{12}(s_{i-2} - 2s_{i-1} + s_i)^2 + \frac{1}{4}(s_{i-2} - 4s_{i-1} + 3s_i)^2,\\
\beta_2 &= \frac{13}{12}(s_{i-1} - 2s_i + s_{i+1})^2 + \frac{1}{4}(s_{i-1} - s_{i+1})^2,\\
\beta_3 &= \frac{13}{12}(s_i - 2s_{i+1} + s_{i+2})^2 + \frac{1}{4}(3s_i - 4s_{i+1} + s_{i+2})^2.
\end{aligned} \tag{34}$$

Here, ε is a parameter to prevent the denominator from becoming 0, and is usually taken as 10^{-6}. Finally, the numerical flux $(\hat{f}_1)_{i+\frac{1}{2}j}$ is given by the following convex combination of the three third-order fluxes (31) as

$$(\hat{f}_1)_{i+\frac{1}{2}j} = \omega_1\hat{s}^{(1)}_{i+\frac{1}{2}} + \omega_2\hat{s}^{(2)}_{i+\frac{1}{2}} + \omega_3\hat{s}^{(3)}_{i+\frac{1}{2}} \tag{35}$$

with the nonlinear weights given by (32).

For the general case where $f_1'(\rho)$ may change sign, first we form a flux splitting $f_1(\rho) = f_1^+(\rho) + f_1^-(\rho)$ such that $\frac{\mathrm{d}}{\mathrm{d}\rho}f_1^+(\rho) \geqslant 0$ and $\frac{\mathrm{d}}{\mathrm{d}\rho}f_1^-(\rho) \leqslant 0$. We then perform the procedure above to obtain the numerical flux corresponding to $f_1^+(\rho)$, and use a mirror symmetric procedure, with respect to the location $x_{i+\frac{1}{2}}$, to obtain the numerical flux corresponding to $f_1^-(\rho)$. These two numerical fluxes are then combined to form the final numerical flux. Several flux splittings are used in practice, and the most common is the Lax–Friedrichs splitting, which is given by

$$f_1^{\pm}(\rho) = \frac{1}{2}(f_1(\rho) \pm \alpha\rho), \quad \text{where } \alpha = \max|f_1'(\rho)| \tag{36}$$

and which is used in our simulation. For our purposes, we take

$$\alpha = \max_i |U(\rho(x_i, y_j, t), x_i, y_j)|. \tag{37}$$

4.2. The fast sweeping WENO method

Before we solve Eq. (26) directly, we first take the norm on both vectors to derive the Eikonal equation (15), which is then solved as an intermediate step. The Eikonal equation is a special case of steady-state Hamilton–Jacobi equations. Solutions to Hamilton–Jacobi equations are usually continuous but not everywhere differentiable, and are usually not unique. We seek an approximation to the viscosity solution (Crandall and Lions, 1983), which is the physically relevant solution for many applications including our model. Numerical solutions for approximating the viscosity solutions of the Hamilton–Jacobi equations follow lines similar to those for solving conservation laws. Thus, the third- and fifth-order WENO schemes for conservation laws designed by Liu et al. (1994) and Jiang and Shu (1996) are extended to WENO schemes for solving the Hamilton–Jacobi equations of Jiang and Peng (2000). Because Eq. (15) is a steady-state equation, if we used the time-dependent WENO scheme of Jiang and Peng (2000), we would need to introduce a pseudo-time and then march to a steady state for each fixed t. This would be a very costly procedure. Therefore, we use the recently developed fast sweeping method of Zhang et al. (2006), which is based on the third-order WENO scheme of Jiang and Peng (2000). This fast sweeping method is much faster in computer time than the pseudo-time marching. We describe this fast sweeping method briefly, and Zhang et al. (2006) can be referred to for more details.

The fast sweeping WENO method starts with the following initialization. Based on the boundary condition $\phi(x,y) = 0$ for $(x,y) \in \Gamma_d$, we assign the exact boundary values on Γ_d. The solution from the first-order Godunov fast sweeping method (Zhao, 2005) is used as the initial guess at all other grid points. The first-order Godunov fast sweeping method is very fast but is less accurate than the high-order WENO scheme. By using its result as the initial guess of the high-order WENO scheme, we can obtain the more accurate high-order WENO result with fewer iterations. For those grid points whose distance to Γ_d is less than or equal to $2h$, we fix their solution values as the initial guess during the iterations.

The following Gauss–Seidel iterations with four alternating direction sweepings are then performed.

$$\begin{aligned} &(1)\ i = 1 : N_x, \quad j = 1 : N_y; \quad (2)\ i = N_x : 1, \quad j = 1 : N_y; \\ &(3)\ i = N_x : 1, \quad j = N_y : 1; \quad (4)\ i = 1 : N_x, \quad j = N_y : 1. \end{aligned} \tag{38}$$

where (i,j) is the grid index pair in (x,y) and N_x and N_y are the number of grid points in x and y, respectively. When we loop to a point (i,j), the solution is updated as follows:

$$\phi_{i,j}^{\text{new}} = \begin{cases} \min(\phi_{i,j}^{x\min}, \phi_{i,j}^{y\min}) + c_{i,j}h, & \text{if } |\phi_{i,j}^{x\min} - \phi_{i,j}^{y\min}| \leqslant c_{i,j}h, \\ \dfrac{\phi_{i,j}^{x\min} + \phi_{i,j}^{y\min} + (2c_{i,j}^2h^2 - (\phi_{i,j}^{x\min} - \phi_{i,j}^{y\min})^2)^{\frac{1}{2}}}{2}, & \text{otherwise}, \end{cases} \tag{39}$$

where $c_{i,j} = C(x_i, y_j, t)$, and

$$\begin{cases} \phi_{i,j}^{x\min} = \min(\phi_{i,j}^{\text{old}} - h(\phi_x)_{i,j}^-, \phi_{i,j}^{\text{old}} + h(\phi_x)_{i,j}^+), \\ \phi_{i,j}^{y\min} = \min(\phi_{i,j}^{\text{old}} - h(\phi_y)_{i,j}^-, \phi_{i,j}^{\text{old}} + h(\phi_y)_{i,j}^+), \end{cases} \tag{40}$$

This is same as usual if the phi^{-} thing is not considered. Which means they are as mentioned in the original paper of fast sweep method.

with

$$(\phi_x)_{i,j}^- = (1 - w_-)\left(\frac{\phi_{i+1,j} - \phi_{i-1,j}}{2h}\right) + w_-\left(\frac{3\phi_{i,j} - 4\phi_{i-1,j} + \phi_{i-2,j}}{2h}\right), \tag{41}$$

We see that here also the indexing of points goes from (i-2) to (i+2), and thus again this is a fifth order method.

$$(\phi_x)_{i,j}^+ = (1 - w_+)\left(\frac{\phi_{i+1,j} - \phi_{i-1,j}}{2h}\right) + w_+\left(\frac{-3\phi_{i,j} + 4\phi_{i+1,j} - \phi_{i+2,j}}{2h}\right), \tag{42}$$

$$w_- = \frac{1}{1 + 2r_-^2}, \quad r_- = \frac{\varepsilon + (\phi_{i,j} - 2\phi_{i-1,j} + \phi_{i-2,j})^2}{\varepsilon + (\phi_{i+1,j} - 2\phi_{i,j} + \phi_{i-1,j})^2}, \tag{43}$$

$$w_+ = \frac{1}{1 + 2r_+^2}, \quad r_+ = \frac{\varepsilon + (\phi_{i,j} - 2\phi_{i+1,j} + \phi_{i+2,j})^2}{\varepsilon + (\phi_{i+1,j} - 2\phi_{i,j} + \phi_{i-1,j})^2}. \tag{44}$$

Notice that (39) and (40) are local solutions of the WENO approximation based on available neighboring data, with a detailed derivation given in Zhang et al. (2006). The nonlinear weights are the same as those in (32), as well as the meaning of ε, only that they are written in a different form as in Jiang and Peng (2000) for easier implementation. The definitions for $(\phi_y)_{i,j}^-$ and $(\phi_y)_{i,j}^+$ are of course analogous.

Convergence is declared if

$$\|\phi^{\text{new}} - \phi^{\text{old}}\| \leqslant \delta, \tag{45}$$

where δ is a given convergence threshold value. We use $\delta = 10^{-9}$ in our computation. The algorithm converges very rapidly in our numerical simulation.

4.3. The third-order TVD Runge–Kutta time discretization

Finally, the semi-discrete scheme (30) must also be discretized in time. We use the third-order total-variation-diminishing (TVD) Runge–Kutta method (Shu and Osher, 1988), which can maintain the stability of the spatial discretization. If we denote the right-hand side of the ordinary differential equation system (30) by $L(\rho)_{i,j}$, then the Runge–Kutta method is given by

$$\begin{aligned}\rho^{(1)} &= \rho^n + \Delta t L(\rho^n),\\ \rho^{(2)} &= \tfrac{3}{4}\rho^n + \tfrac{1}{4}(\rho^{(1)} + \Delta t L(\rho^{(1)})),\\ \rho^{n+1} &= \tfrac{1}{3}\rho^n + \tfrac{2}{3}(\rho^{(2)} + \Delta t L(\rho^{(2)})).\end{aligned} \tag{46}$$

4.4. Solution procedure

The main time evolution equation to be solved is Eq. (24). When the flux function $\mathbf{f}$ is known, this is a scalar two-dimensional hyperbolic conservation law. We use the fifth-order finite difference WENO scheme that is described in Section 4.1. Time discretization is accomplished by the third-order total-variation-diminishing (TVD) Runge–Kutta method that is described in Section 4.3.

We use a uniformly spaced mesh denoted by x_i, $i = 1,\ldots,N_x$ and y_j, $j = 1,\ldots,N_y$. The uniform mesh sizes in the x and y directions are denoted by Δx and Δy, respectively. The mesh points are arranged such that the physical boundary of the domain (entrance, exit, and walls) is located at the midpoint between two grid points. For example, if the bottom wall is at $y = 0$, then the first grid point inside the computational domain is $y_1 = \frac{1}{2}\Delta y$, and the first "ghost point" outside of the computational domain is $y_0 = -\frac{1}{2}\Delta y$. Note that some of the grid points might be in the region of the obstruction (see the following section for more details), so the solutions at those grid points are meaningless and do not need to be updated. We also need values of the solution at some of the ghost points, namely, those points (x_i, y_j) that are outside the computational domain or inside the region of the obstruction. The solution $\rho_{i,j}$ and the flux $\mathbf{f}_{i,j} = ((f_1)_{i,j},(f_2)_{i,j})$ denote the approximations to ρ and $\mathbf{f}$ at the grid point (x_i, y_j). The Euler forward time discretization for Eq. (30) is given by

$$\rho_{i,j}^{n+1} = \rho_{i,j}^{n} - \frac{\Delta t}{\Delta x}\left((\hat{f}_1)_{i+\frac{1}{2},j} - (\hat{f}_1)_{i-\frac{1}{2},j}\right) - \frac{\Delta t}{\Delta y}\left((\hat{f}_2)_{i,j+\frac{1}{2}} - (\hat{f}_2)_{i,j-\frac{1}{2}}\right), \tag{47}$$

where the superscript n denotes the time level, and the numerical fluxes $(\hat{f}_1)_{i+\frac{1}{2},j}$ and $(\hat{f}_2)_{i,j+\frac{1}{2}}$ are computed from the point values $\rho_{i,j}$ and fluxes $\mathbf{f}_{i,j}$ using the fifth-order accurate finite difference WENO procedure based on Lax–Friedrichs flux splitting, as described in Section 4.1. The specific boundary conditions that are used for our test case are described in the following section. Finally, the third-order TVD Runge–Kutta method is a convex combination of three Euler forward steps given by (46).

To compute the fluxes $\mathbf{f}_{i,j}$ by Eq. (26), we need to find the potential ϕ using Eq. (15) when the cost function is $c(x,y,t)$. We use the third-order accurate WENO scheme described in Section 4.2 to discretize the Eikonal equation (15). The scheme takes the form

$$\hat{H}((\phi_x)^-_{i,j}, (\phi_x)^+_{i,j}; (\phi_y)^-_{i,j}, (\phi_y)^+_{i,j}) = c(x_i, y_j, t^n), \tag{48}$$

where $\hat{H}$ is the Godunov type monotone Hamiltonian, and $(\phi_x)^{\pm}$ and $(\phi_y)^{\pm}$ are the WENO approximations of the left and right derivatives of ϕ in the x and y directions. We then use the fast sweeping method with the third-order WENO scheme discussed in Section 4.2 to solve the problem. The boundary conditions are explained in the following section.

In summary, starting from the density ρ^n at time level n, we obtain the density ρ^{n+1} by the following steps in an Euler forward time discretization.

1. Obtain the cost function c by formula (12);
2. Solve the Eikonal equation (15) by a third-order WENO discretization using the fast sweeping method to obtain ϕ;
3. Obtain the magnitude $||\mathbf{f}||$ of the flux $\mathbf{f}$ by using formula (25);
4. Obtain the flux $\mathbf{f}$ by using formula (26); and
5. Use the fifth-order Lax–Friedrichs WENO scheme to obtain ρ^{n+1} by solving the conservation law (24).

The third-order TVD Runge–Kutta time discretization is then just a convex combination of three Euler forward steps. Then, the procedure repeats until it marches to the end of the analysis period.

5. Numerical example

Consider a railway platform that is 100 m long and 50 m wide, as shown in Fig. 1. Pedestrians enter the platform from the left boundary, which has a width of 50 m, and leave at either of the two exit gates on the right boundary, each of which has an exit width of 15 m. There is an obstruction 20 m by 20 m in the middle of the platform.

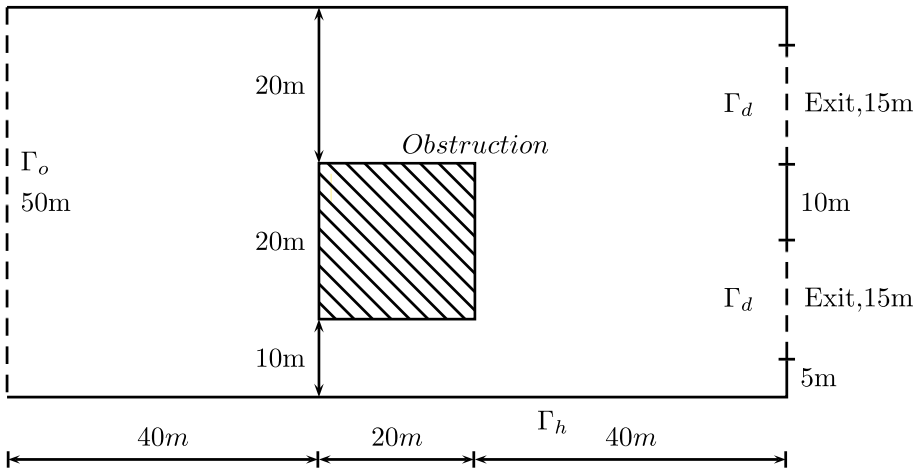

Fig. 1. The geometry of the railway platform.

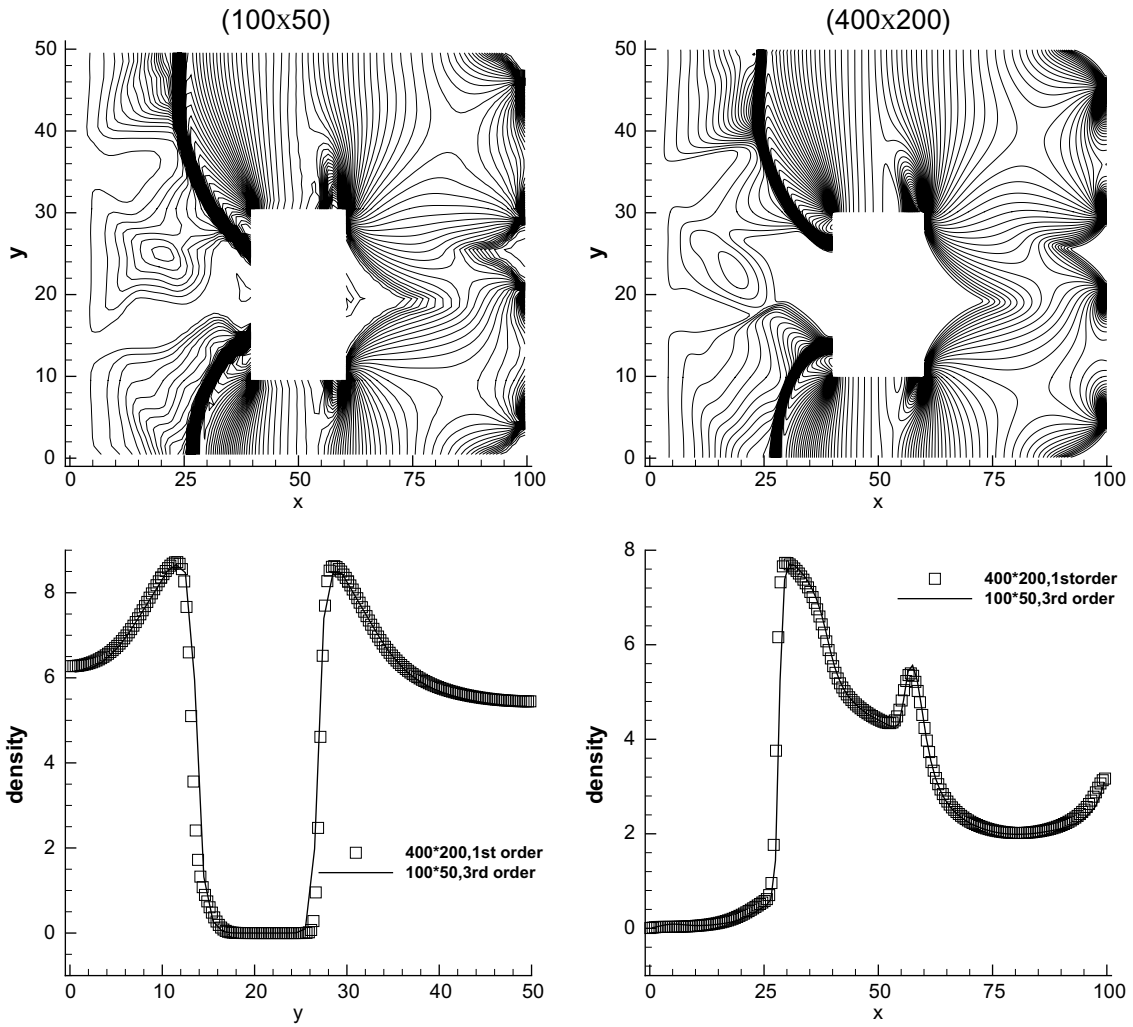

Fig. 2. Density ρ at $t = 120$ s. Top: 90 equal speed contours from $\rho_{min} = 0.0$ to $\rho_{max} = 9.5$, by the high-order WENO scheme using a 100×50 uniform mesh (left), and by the first-order scheme using a 400×200 uniform mesh (right). A comparison of the one-dimensional cuts at $x = 36$ m (bottom left) and at $y = 33$ m (bottom right) is also given, where the solid lines are obtained by the high-order WENO scheme with a 100×50 mesh, and the symbols are obtained by the first-order scheme with a 400×200 mesh.

The study horizon is 300 s. The time-varying demand increases linearly from zero to a peak of five pedestrians per meter per second at $t = 60$ s, and then drops linearly back to zero at $t = 120$ s, and no pedestrian crosses the boundary thereafter. According to Eq. (27), the boundary condition that represents the time-varying demand is expressed as

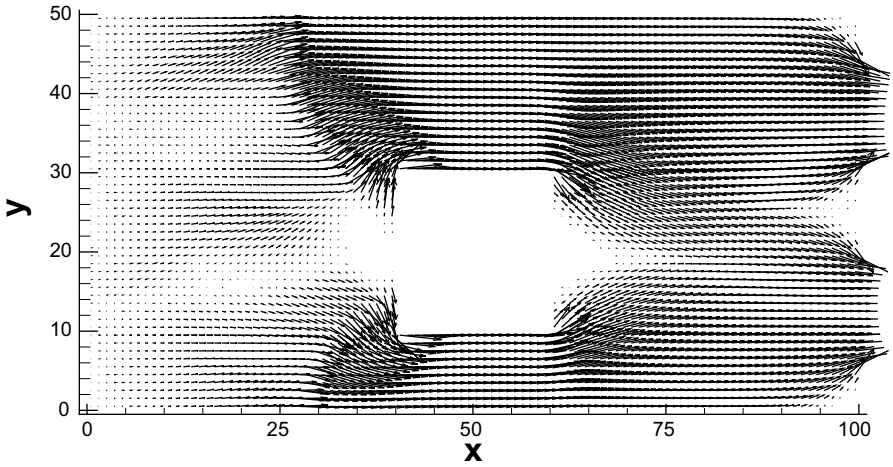

Fig. 3. The flow vector **f** at $t = 120$ s.

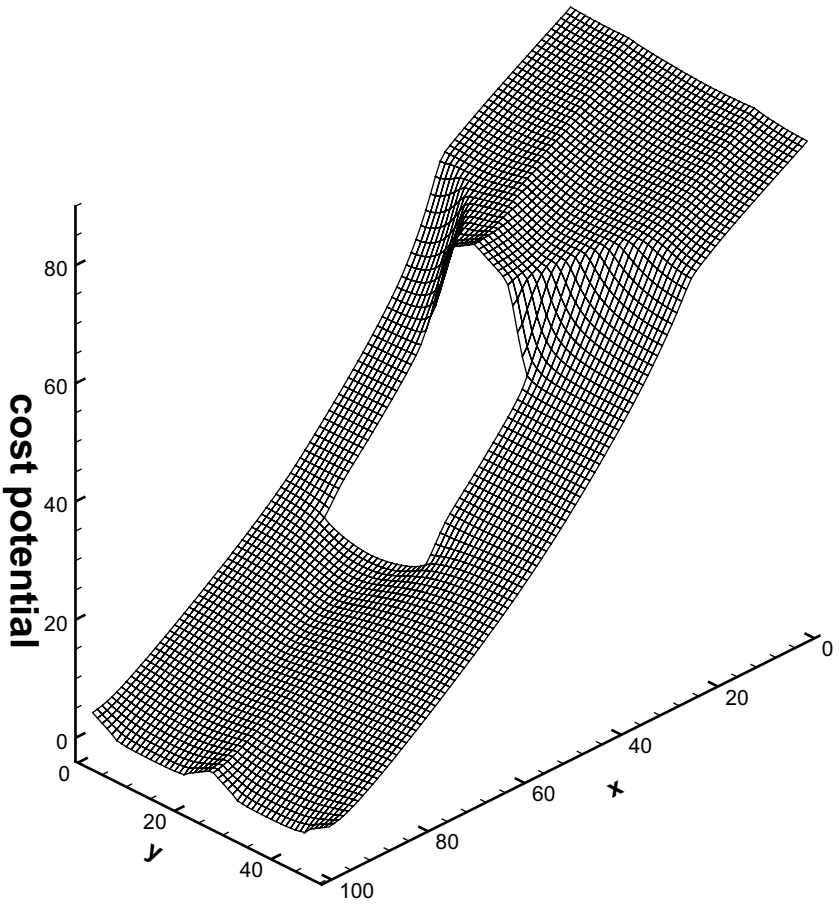

Fig. 4. The cost potential ϕ at $t = 120$ s.

$$f_1(0,y,t) = \begin{cases} t/12 & 0 \leqslant t \leqslant 60, \\ 10 - t/12 & 60 \leqslant t \leqslant 120, \\ 0 & 120 \leqslant t \leqslant 0, \end{cases}$$

$$f_2(0,y,t) = 0 \quad \forall y \in (0,50), \ \ t \in (0,300),$$

where the flow is expressed in ped/m/s. Initially, the railway platform is empty, i.e., $\rho_0(x,y) = 0 \ \forall (x,y) \in \Omega$, at $t = 0$. We assume a linear speed–density relationship (analogous to Greenshields' traffic flow model of a homogeneous highway) for the whole platform

$$U(\rho) := 2(1 - \rho/10),$$

where the speed is expressed in m/s, and the density in ped/m^2. The maximum free-flow speed is 2 m/s, and the maximum density is 10 ped/m^2. In addition, we define a discomfort function

$$G(\rho) := 0.002\rho^2,$$

where the level of discomfort increases with the density, and is expressed in equivalent time unit. Note that when the density is zero, the platform is empty and thus a pedestrian can walk freely on the platform without being affected by another

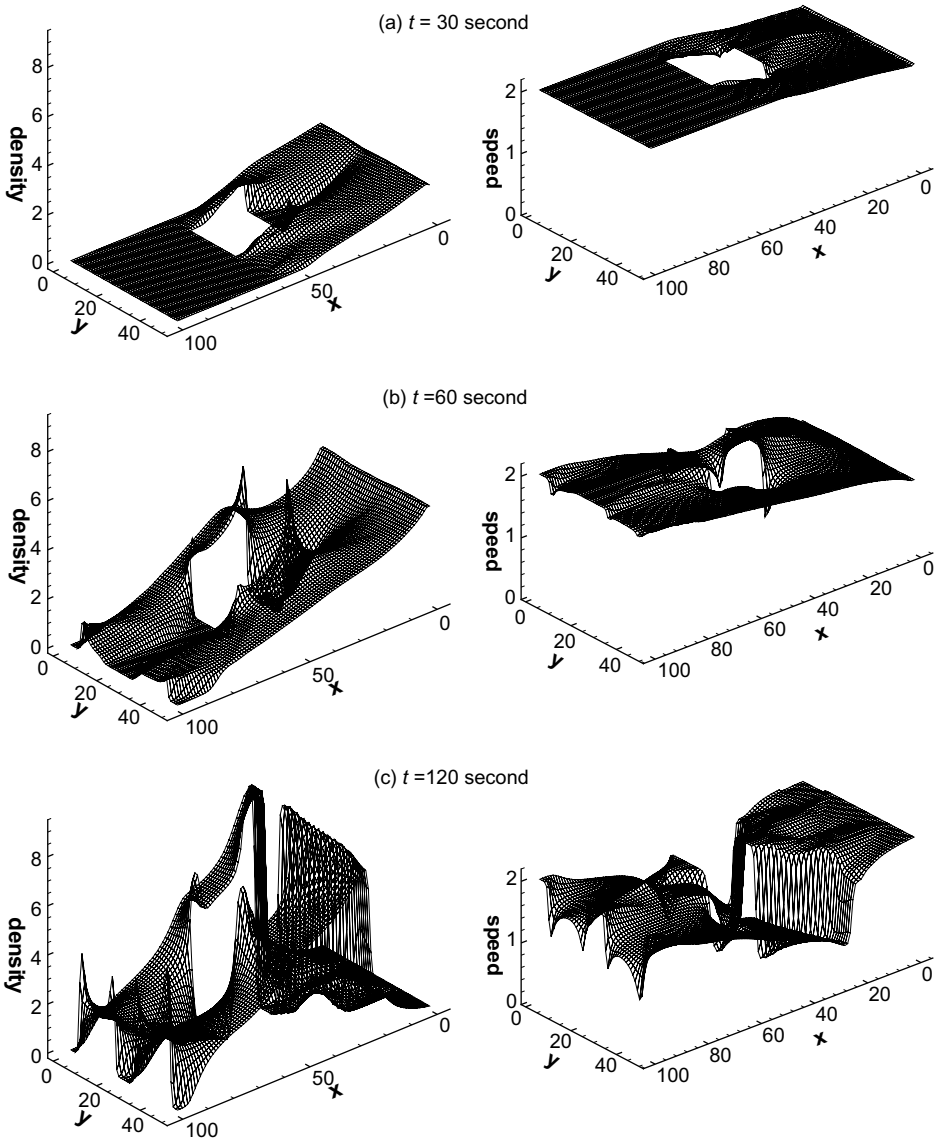

Fig. 5. The density ρ (left) and the velocity u (right) at different times: (a) $t = 30$ s; (b) $t = 60$ s; (c) and $t = 120$ s. The density ρ (left) and the velocity u (right) at different times: (d) $t = 180$ s and (e) $t = 240$ s.

pedestrian. In that case, the discomfort function vanishes. The walking cost is taken as the sum of the walking time and the level of discomfort in the equivalent time unit on the railway platform, and is assumed to be location and time independent. Hence, we have

$$C(\rho) = \frac{1}{2(1-\rho/10)} + 0.002\rho^2.$$

We now use the WENO algorithm that is described in the previous section to perform the numerical simulation. The computational domain $[0,100] \times [0,50]$ (units: m) is covered with a uniform mesh with a $N_x \times N_y$ grid. The mesh points inside the obstruction $[40,60] \times [10,30]$ are excluded from the computation. The numerical boundary conditions are implemented as follows.

1. On the inflow boundary Γ_o, namely, at $x = 0$, $0 \leqslant y \leqslant 50$, the flux $\mathbf{f}$ is prescribed. As $x = 0$ is in the middle of two grid points x_0 and x_1, it is the location at which a numerical flux $(\hat{f}_1)_{\frac{1}{2}}$ is needed. We then simply set $(\hat{f}_1)_{\frac{1}{2}} = 0$. The boundary conditions for ρ and ϕ are obtained by extrapolation from inside the computational domain.
2. On the solid wall boundary Γ_h, namely, the top, bottom, and part of the right boundary and the boundary of the obstruction, we set the normal flux of $\mathbf{f}$ to be zero. Again, as all such boundaries are located in the middle of two grid points, the normal numerical flux is needed there, and we simply set it to zero. The values of ρ at the ghost points inside the wall are set to zero, and those of ϕ are set to 10^{12}.
3. On the outflow boundary Γ_d, namely, at $x = 100$, $5 \leqslant y \leqslant 20$, and $30 \leqslant y \leqslant 45$, we set $\phi = 0$. The values of ρ at the ghost points are obtained by extrapolation from inside the computational domain.

We also performed simulations using first-order accurate numerical solvers (the first-order Lax–Friedrichs scheme for the conservation law (24) and the first-order Godunov type scheme for the Eikonal equation (15)). The numerical results of the first-order scheme with a 400×200 grid are comparable to those of the high-order WENO scheme with a 100×50 grid (see Fig. 2). For this example, the computing time of the first-order scheme with a 400×200 grid is comparable to that of the high-order WENO scheme using a 100×50 grid, but the first-order scheme uses much more memory space. For more complex problems, it is expected that the high-order WENO scheme may save computational costs and achieve a resolution comparable to that of the first-order scheme. We present the numerical results of the high-order WENO scheme with a 100×50 grid in the following figures.

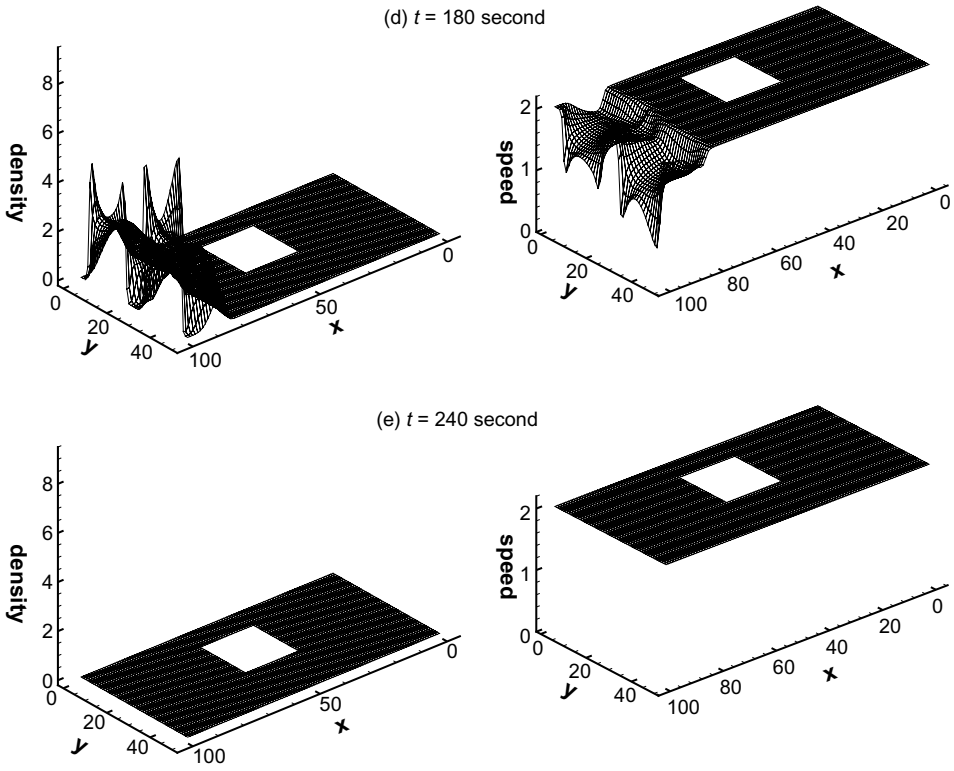

Fig. 5 (*continued*)

In Fig. 3, we plot the flow vector **f** at time $t = 120$ (unit: second), which shows the movement pattern of pedestrians who move around the obstacle in the middle of the platform and head to the exits. In conjunction with Fig. 2, two shocks are clearly seen before the obstruction due to the reduction in the width of the corridor. Such shocks are frequently observed in a walking facility with large crowds when pedestrians queue up to walk through a bottleneck with reduced capacity. Three triangular vacuum regions in front of and behind the obstacle, and between the two exits, are also observed, which is consistent with the travel cost minimization strategy of the pedestrians. Fig. 4 shows the cost potential at $t = 120$, which depicts the instantaneous travel cost from a given location to the exit of the platform. We clearly observe the sharp increase in travel cost across the two shocks before the obstruction, which are caused by the pedestrian queues that prevent pedestrians from moving forward. Note that these shocks are dynamic and their locations change with time, as further revealed in the sequel.

Fig. 5 shows the density ρ (left) and the velocity u (right) at $t = 30$, 60, 120, 180, and 240. This helps to illustrate the evolution of the congestion pattern on the railway platform. The propagation of the congestion wave as reflected by the speed drop is revealed by this series of plots. Near the end of the study period (i.e., $t = 240$), all pedestrians have left the platform, and the traffic condition returns to the free-flowing situation with a speed of 2 m/s for the whole platform. We can observe that relatively higher density concentrations occur locally near the corners of the square obstruction and the edges of the two exits, which indicates that the geometry of the platform is not optimal for pedestrian flows. Curved (round) walls and obstacles might yield smoother and lower density distribution that provides a better walking environment for pedestrians.

To further illustrate the evolution of the flow intensity within the critical section of the platform on both sides of the obstacle, Fig. 6 plots the flow **f** at $x = 50$ for $t = 30$, 60, 120, and 180. The flow initially increases steadily, but reaches a maximum (capacity) at the end of the peak period at $t = 120$. The pedestrian traffic clears before $t = 180$, as depicted in Fig. 5, which shows that the pedestrians have already left the region of the obstruction. Fig. 7 shows a similar graph at $x = 90$ near

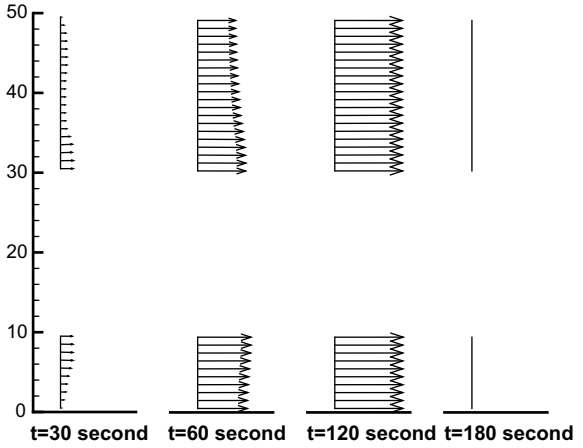

Fig. 6. The flow vector **f** at $t = 30$, 60, 120, and 180 s and at $x = 50$ m.

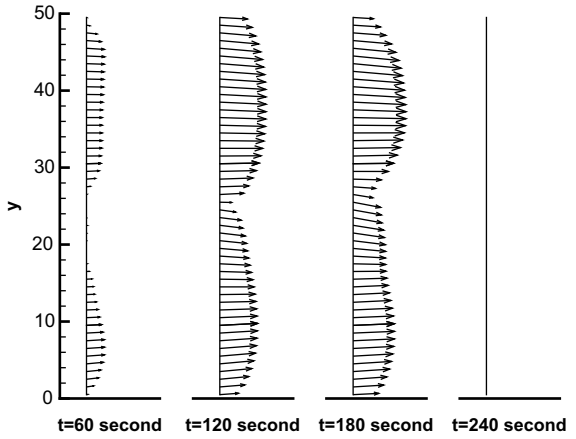

Fig. 7. The flow vector **f** at $t = 60$, 120, 180, and 240 s and at $x = 90$ m.

the two exits that illustrates that the upper exit attracts a higher flow because of the obstruction that is placed towards the bottom boundary.

6. Conclusions

We have revisited Hughes' dynamic continuum model for pedestrian flow in a two-dimensional walking facility that is represented as a continuum within which pedestrians can freely move in any direction (Hughes, 2002). We have first reformulated Hughes' model, and then shown that the pedestrian route choice strategy in Hughes' model satisfies the reactive dynamic user equilibrium principle in which a pedestrian chooses a route to minimize the instantaneous travel cost to the destination. In this model, the pedestrian demand is time varying. The pedestrian density, flux, and walking speed are governed by a conservation equation. A generalized cost function has been considered. We have also derived an efficient solution algorithm, which uses state-of-the-art methods for solving different sub-problems, such as the efficient weighted essentially non-oscillatory (WENO) scheme for the conservation equation and the fast sweeping method for the Eikonal equation. A numerical example has been used to demonstrate the effectiveness of the proposed solution procedure.

This model will provide a useful tool for the planning and design of walking facilities. The results will help in the visualization of the evolution of the level of service of the walking facility, and the reporting of the movement trajectories of pedestrians and their interactions within the walking facility, which will be useful for the evaluation of the effectiveness of the facility design and the identification of critical locations that need special attention. In addition, there are several promising research directions.

First, we have considered a single commodity of pedestrian flow in the paper. However, if there are multiple origins and multiple destinations, the problem becomes a multi-commodity problem for which a better understanding is needed of pedestrian behavior in conflicting streams with different directions in a two-dimensional space. Experiments are now being undertaken to extract such behavior, which will be used to develop a multi-commodity pedestrian flow model through which we will be able to explain the changes in the capacity with respect to different pedestrian flow directions. Second, while the predictive user equilibrium model is suitable for more strategic behavior modeling, the reactive user equilibrium model is useful for representing pedestrian behavior at an operational level. However, it would be interesting to combine both reactive and predictive user equilibrium principles in a systematic framework, forming a mixed route choice strategy to model the flow of pedestrians with patterns of exploratory behavior by the reactive approach and the flow of pedestrians with repetitive behavior having full information of the operating conditions of the walking facility by the predictive approach. Third, it would be useful to conduct observational surveys to obtain pedestrian flow information to calibrate and validate the proposed model. Fourth, it would also be challenging to extend the work to deal with some interesting phenomena, such as the capacity of an open door is higher than the capacity of a narrow hall of the same width because to pass through the open door, pedestrians will rotate their body for easy passage, which increases the effective capacity of the door compared to that of a narrow hall, and the well-known faster-is-slower effect causing (temporarily) blockades due to arc formation at the bottleneck.

Although the model and numerical solution approach are applied to pedestrian flows in this paper, the methodology can also be applied to an urban transportation system for which we consider a city with several highly compact central business districts (CBDs). Commuter origins are continuously dispersed over the whole city and travel demand is time varying. The dense transportation network system can be approximated as a continuum in which users are free to choose their routes in a two-dimensional space, based on the major assumption that the differences between adjacent areas within a network are relatively small when compared to the variation over the entire network, and hence the characteristics of the network can be represented by smooth mathematical functions (Vaughan, 1987). During a peak period, if we assume commuters receive real-time traffic information through a radio broadcast, mobile phone, or in-vehicle navigation unit, based on which they make dynamic route choice decisions in a reactive manner, then we can apply this model for the prediction of macroscopic traffic congestion in an urban area. This is an interesting area for future research.

Acknowledgements

The research of the second author was supported by a grant from the Research Grants Council of the Hong Kong Special Administrative Region, China (HKU 7176/07E). The research of the third author was supported by the Chinese Academy of Sciences Grant 2004-1-8. The research of the fourth author was supported by the Chinese Academy of Sciences during his visit to the University of Science and Technology of China (Grant 2004-1-8) and to the Institute of Computational Mathematics and Scientific/Engineering Computing. Additional support was provided by ARO Grant W911NF-04-1-0291 and NSF Grant DMS-0510345. The research of the fifth author was supported by a grant from the Research Grants Council of the Hong Kong Special Administrative Region, China (PolyU 5168/04E).

References

Al-Masaeid, H.R., Al-Suleiman, T.I., Nelson, D.C., 1993. Pedestrian speed–flow relationship for central business district areas in developing countries. Transportation Research Record 1396, 69–74.

Buckman, L.T., Leather, J.A., 1994. Modelling station congestion the PEDROUTE way. Traffic Engineering and Control 35 (6), 373–377.

Cheung, C.Y., Lam, W.H.K., 1998. Pedestrian route choices between escalator and stairway in MTR stations. ASCE Journal of Transportation Engineering 124 (3), 277–285.
Crandall, M., Lions, P.L., 1983. Viscosity solutions of Hamilton–Jacobi equations. Transactions of American Mathematical Society 277 (1), 1–42.
Daly, P.N., McGrath, F., Annesley, T.J., 1991. Pedestrian speed/flow relationships from underground stations. Traffic Engineering and Control 32 (2), 75–78.
Dernellis, A., Ashworth, R., 1994. Pedestrian subways in urban areas: some observations concerning their use. Traffic Engineering and Control 35 (1), 14–18.
Gaskell, G.D., Benewick, R.J., 1987. The Crowd in Contemporary Britain. Sage Publications Ltd., London.
Harris, N.G., 1991. Modelling walk link congestion and the prioritization of congestion relief. Traffic Engineering and Control 32 (2), 78–80.
Helbing, D., Buzna, L., Johansson, A., Werner, T., 2005. Self-organized pedestrian crowd dynamics: experiments, simulations, and design solutions. Transportation Science 39 (1), 1–24.
Ho, H.W., Wong, S.C., 2007. Housing allocation problem in a continuum transportation system. Transportmetrica 3 (1), 21–39.
Ho, H.W., Wong, S.C., Hau, T.D., 2007. Existence and uniqueness of a solution for the multi-class user equilibrium problem in a continuum transportation system. Transportmetrica 3 (2), 107–117.
Ho, H.W., Wong, S.C., Loo, B.P.Y., 2004. Sequential optimization approach for the multi-class user equilibrium problem in a continuous transportation system. Journal of Advanced Transportation 38 (3), 323–345.
Ho, H.W., Wong, S.C., Loo, B.P.Y., 2006. Combined distribution and assignment model for a continuum traffic equilibrium problem with multiple user classes. Transportation Research Part B 40 (8), 633–650.
Ho, H.W., Wong, S.C., Yang, H., Loo, B.P.Y., 2005. Cordon-based congestion pricing in a continuum traffic equilibrium system. Transportation Research Part A 39 (7–9), 813–834.
Hoogendoorn, S.P., Bovy, P.H.L., 2004a. Pedestrian route-choice and activity scheduling theory and models. Transportation Research Part B 38 (2), 169–190.
Hoogendoorn, S.P., Bovy, P.H.L., 2004b. Dynamic user-optimal assignment in continuous time and space. Transportation Research Part B 38 (7), 571–592.
Hoogendoorn, S.P., Bovy, P.H.L., Daamen, W., 2003. Walking infrastructure design assessment by continuous space dynamic assignment modeling. Journal of Advanced Transportation 38 (1), 69–92.
Hughes, R.L., 2002. A continuum theory for the flow of pedestrians. Transportation Research Part B 36 (6), 507–535.
Jiang, G., Peng, D.P., 2000. Weighted ENO schemes for Hamilton–Jacobi equations. SIAM Journal on Scientific Computing 21 (6), 2126–2143.
Jiang, G., Shu, C.W., 1996. Efficient implementation of weighted ENO schemes. Journal of Computational Physics 126 (1), 202–228.
Koushki, P.A., Ali, S.Y., 1993. Pedestrian characteristics and the promotion of walking in Kuwait city center. Transportation Research Record 1396, 30–33.
Lam, W.H.K., Cheung, C.Y., 1997. A study of the bi-directional pedestrian flow characteristics in Hong Kong Mass Transit Railway stations. Journal of Eastern Asia Society for Transportation Studies 2, 1607–1620.
Lam, W.H.K., Cheung, C.Y., 1998. Pedestrian travel time functions for the Hong Kong underground stations: calibration and validation. Hong Kong Institution of Engineers Transactions 5 (3), 39–45.
Lam, W.H.K., Cheung, C.Y., 2000. Pedestrian speed/flow relationships for walking facilities in Hong Kong. ASCE Journal of Transportation Engineering 126 (4), 343–349.
Lam, W.H.K., Cheung, C.Y., Lam, C.F., 1999. A study of crowding effects at the Hong Kong light rail transit stations. Transportation Research Part A 33 (5), 401–415.
Lam, W.H.K., Lee, J.Y.S., Cheung, C.Y., 2002. A study of the bi-directional pedestrian flow characteristics at Hong Kong signalized crosswalk facilities. Transportation 29 (2), 169–192.
Lam, W.H.K., Lee, J.Y.S., Lee, K.S., Goh, P.K., 2003a. A generalised function for modeling bi-directional flow effects on indoor walkways in Hong Kong. Transportation Research Part A 37 (9), 789–810.
Lam, W.H.K., Morrall, J.F., Ho, H., 1995. Pedestrian flow characteristics in Hong Kong. Transportation Research Record 1487, 56–62.
Lam, W.H.K., Tam, M.L., Wong, S.C., Wirasinghe, S.C., 2003b. Wayfinding in the passenger terminal of Hong Kong International Airport. Journal of Air Transport Management 9 (2), 73–81.
LeVeque, R.J., 1992. Numerical Methods for Conservation Laws. Lecture in Mathematics. Birkhauser-Verlag, Basel, ETH Zurich, Switzerland.
Lighthill, M.J., Whitham, G.B., 1955. On kinetic wave II: a theory of traffic flow on crowded roads. Proceedings of the Royal Society of London, Series A 229 (1178), 317–345.
Liu, X.-D., Osher, S., Chan, T., 1994. Weighted essentially nonoscillatory schemes. Journal of Computational Physics 115 (1), 200–212.
Loo, B.P.Y., Ho, H.W., Wong, S.C., 2005. An application of the continuous equilibrium modelling approach in understanding the geography of air passenger flows in a multi-airport region. Applied Geography 25 (2), 169–199.
Morrall, J.F., Ratnayake, L.L., Seneviratne, P.N., 1991. Comparison of central business district pedestrian characteristics in Canada and Sri Lanka. Transportation Research Record 1294, 57–61.
Richards, P.I., 1956. Shock waves on the highway. Operations Research 4 (1), 42–51.
Selim, S.Z., Al-Rabeh, A.H., 1991. On the modeling of pedestrian flow on the Jamarat bridge. Transportation Science 25 (4), 257–263.
Setti, J.R., Hutchinson, B.J., 1994. Passenger-terminal simulation model. ASCE Journal of Transportation Engineering 120 (4), 517–535.
Shu, C.-W., 2003. High-order finite difference and finite volume WENO schemes and discontinuous Galerkin methods for CFD. International Journal of Computational Fluid Dynamics 17 (2), 107–118.
Shu, C.W., Osher, S., 1988. Efficient implementation of essentially non-oscillatory shock-capturing schemes. Journal of Computational Physics 77 (2), 439–471.
Tanaboriboon, Y., Guyano, J.A., 1991. Analysis of pedestrian movements in Bangkok. Transportation Research Record 1294, 52–56.
Tong, C.O., Wong, S.C., 2000. A predictive dynamic traffic assignment model in congested capacity-constrained road networks. Transportation Research Part B 34 (8), 625–644.
Vaughan, R.J., 1987. Urban Spatial Traffic Patterns. Pion, London.
Virkler, M.R., Elayadath, S., 1994. Pedestrian speed–flow–density relationships. Transportation Research Record 1438, 51–58.
Wong, S.C., 1994. An alternative formulation of D'Este's trip assignment model. Transportation Research Part B 28 (3), 187–196.
Wong, S.C., 1998. Multi-commodity traffic assignment by continuum approximation of network flow with variable demand. Transportation Research Part B 32 (8), 567–581.
Wong, S.C., Du, Y.C., Ho, H.W., Sun, L.J., 2003. A simultaneous optimization formulation of a discrete/continuous transportation system. Transportation Research Record 1857, 11–20.
Wong, S.C., Lee, C.K., Tong, C.O., 1998. Finite element solution for the continuum traffic equilibrium problems. International Journal for Numerical Methods in Engineering 43 (7), 1253–1273.
Wong, S.C., Sun, S.H., 2001. A distribution and assignment model for continuous facility location problem. Annals of Regional Science 35 (2), 267–281.
Wong, S.C., Yang, H., 1999. Determining market areas captured by competitive facilities: a continuous equilibrium modeling approach. Journal of Regional Science 39 (1), 51–72.
Wong, S.C., Zhou, C.W., Lo, H.K., Yang, H., 2004. An improved solution algorithm for the multi-commodity continuous distribution and assignment model. ASCE Journal of Urban Planning and Development 130 (1), 14–23.
Yang, H., Wong, S.C., 2000. A continuous equilibrium model for estimating market areas of competitive facilities with elastic demand and market externalities. Transportation Science 34 (2), 216–227.
Zhang, M., Shu, C.W., Wong, G.C.K., Wong, S.C., 2003. A weighted essentially non-oscillatory numerical scheme for a multi-class Lighthill–Whitham–Richards traffic flow model. Journal of Computational Physics 191 (2), 639–659.
Zhang, Y.T., Zhao, H.K., Qian, J., 2006. High order fast sweeping methods for static Hamilton–Jacobi equations. Journal of Scientific Computing 29 (1), 25–56.
Zhao, H.K., 2005. A fast sweeping method for Eikonal equations. Mathematics of Computation 74 (250), 603–627.